JOURNAL OF MATERIALS SCIENCE 33 (1998) 2457–2462

Tertiary creep and creep fracture in mechanically alloyed Al–C–O alloys

F. DOBEŠ
Institute of Physics of Materials, Academy of Sciences of the Czech Republic, 61662 Brno, Czech Republic
E-mail: dobes@ipm.cz

The tertiary creep and creep fracture of a set of four mechanically alloyed aluminium alloys with different contents of oxygen and carbon were studied at 623 and 723 K. At low applied stress, the strain to fracture is low, the time to fracture is power-law dependent upon the applied stress, and the specimens fail by intergranular fracture. At high applied stress, the development of a pronounced tertiary stage is observed, the elongation to fracture is increased, the time to fracture is exponentially dependent upon the applied stress, and the fracture appearance is transgranular. The transition stress decreases with increasing temperature and volume fraction of the secondary phases. Analysis of the tertiary creep in the high-stress region leads to the conclusion that the necessary condition for fracture is given by the achievement of a critical fraction of damaged area.

1. Introduction

Although the potential capabilities of aluminium composites with the matrix strengthened by particles of oxides or carbides have been recognized for a long time, practical application of this class of alloys has been approached relatively recently by introducing new technologies, such as mechanical alloying or reaction milling [1, 2]. Consequently, the alloys have attracted the attention of materials scientists, who have focused mainly on the mechanism of the creep deformation [3]. Far less consideration has been given to the accompanying fracture processes. The improved resistance to plastic deformation can be effectively complemented by improved resistance to creep fracture. It has been suggested that the good wettability of oxides in aluminium is the reason for the absence of the nucleation sites that would lead to creep cavities [4]. The specific grain structure with a low proportion of grain boundaries perpendicular to the extrusion axis may also have a retarding effect on the diffusional growth of creep cavities.

The present paper reports a more extensive study of mechanically alloyed aluminium alloys with varying contents of oxygen and carbon. Previous papers [5, 6] were devoted to various aspects of the plastic deformation in the primary and the secondary stages of creep. This paper presents values of the time to the occurrence of fracture, t_f, and the strain required to cause fracture, ε_f, together with the analysis of the tertiary stage of creep.

2. Experimental procedure

Four Al–C–O mechanically alloyed materials were supplied by Erbslöh, Germany. They were prepared by milling aluminium powder with graphite in an attritor under an argon atmosphere, compressing the mixture isostatically while cold, and finally extruding it hot. The alloys AlC0, AlC1 and AlC2 contained nominally 0.8 wt % O_2 and, respectively, 0, 1 and 2 wt % C. The alloy AlC2O2 contained 2 wt % O_2 and 2 wt % C. The structures of the alloys are described in detail elsewhere [6]. Cylindrical specimens, 50 mm in gauge length and 5 mm diameter, were machined from the extruded bars. The specimens were tested under constant applied tensile stress in the range 20–180 MPa at the constant temperatures 623 and 723 K. The creep strain was measured with a sensitivity of 10^{-5}. The creep testing apparatus is described elsewhere [7].

3. Results

At 623 K and low applied stress, the creep curves exhibited a long primary stage, while the secondary and tertiary stages were not pronounced and the strain to fracture was low (~1%). With increased applied stress, the elongation required to achieve fracture was increased rather substantially, the primary creep stage was diminished and the development of a pronounced tertiary stage was observed. The influence of the applied stress on the course of the creep curve is illustrated in Fig. 1. At 723 K, the increased elongation before fracture with increased applied stress is apparent only for the alloys AlC0 and AlC1. The alloys AlC2 and AlC2O2 show an extensive primary stage and an elongation before fracture not exceeding 1%. Higher contents of carbon and oxygen thus appear to decrease the fracture ductility of the alloys. The fracture appearance

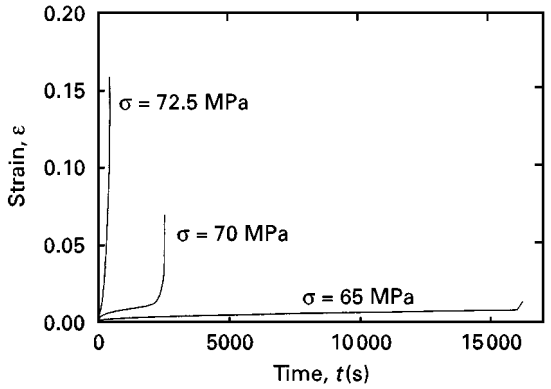

Figure 1 Examples of creep curves in AlC1 at $T = 623$ K.

at low stress is intercrystalline, whereas at high stress it is transcrystalline.

Creep curves without the primary stage can be described on the basis of power [8], exponential [9] or logarithmic functions [10]

$$\varepsilon_{III} = \dot{\varepsilon}_{min} t + At^g \quad (1)$$

$$\varepsilon_{III} = \theta_3(\exp[\theta_4 t] - 1) \quad (2)$$

$$\varepsilon_{III} = -(\ln[1 - C\dot{\varepsilon}_{min} t])/C \quad (3)$$

wherein $\dot{\varepsilon}_{min}$ is the minimum creep rate and A, g, θ_3, θ_4 and C are parameters. Creep curves at higher applied stress which have a pronounced tertiary stage can be successfully described by all three equations. The residual sum of the squares is the least for Equation 1, which is not surprising because of the higher number of calculated parameters. The value of the calculated power $g(g = 7–10)$ is higher than was proposed by Graham and Walles [8] ($g = 3$). The differences between results achieved by using Equations 2 and 3 are small, and Equation 3 is usually to be preferred. Equation 2 can be rewritten as

$$\varepsilon_{III} = (\exp[c\dot{\varepsilon}_{min} t] - 1)/c \quad (4)$$

The values of $\dot{\varepsilon}_{min}$ for both Equations 3 and 4 correspond rather well to the values of the minimum creep rate read directly from the creep curves presented in a previous paper [5]. The values of the parameters c and C are given in Figs 2 and 3. They decrease with both increased stress and increased temperature.

Fig. 4 summarizes the applied stress dependence of the time to fracture, t_f. The times to the occurrence of fracture observed in the alloy AlC2 correspond very well to those reported by Matsuda and Matsuura [11] for a similar mechanically alloyed material with a slightly higher nominal oxygen content. The times to fracture for carbon-deficient alloy (AlC0) are comparable to those reported for an aluminium composite strengthened with silicon carbide particulates (20 vol %) [12]. The applied stress and the temperature dependence of t_f can be characterized by the parameter of applied stress sensitivity, n_f, and the apparent activation energy, Q_f, corresponding to the equation

$$t_f = A_f \sigma^{-n_f} \exp\left(\frac{Q_f}{kT}\right) \quad (5)$$

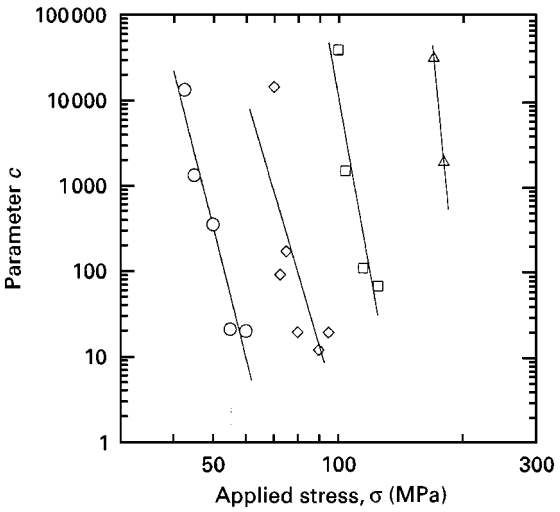

Figure 2 Stress dependence of parameter c in Equation 4, at 623 K: (○) AlC0, (◇) AlC1, (□) AlC2, (△) AlC2O2.

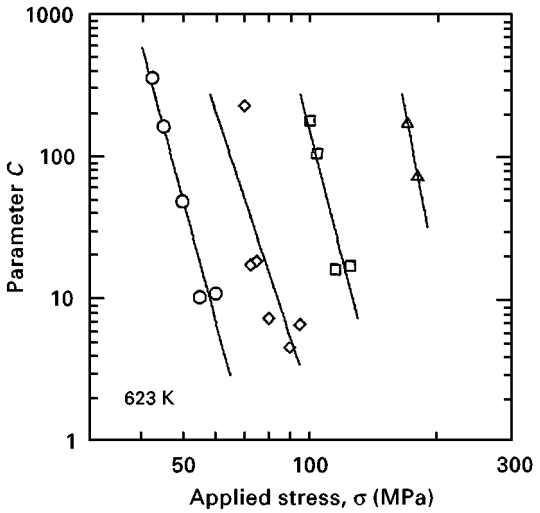

Figure 3 Stress dependence of parameter C in Equation 3, at 623 K: (○) AlC0, (◇) AlC1, (□) AlC2, (△) AlC2O2.

where k is the Boltzmann constant and T is the absolute temperature. The values of n_f in Table I indicate a high applied stress sensitivity that is dependent on the chemical composition of the alloy. The stress sensitivity of t_f is systematically weaker than that of $\dot{\varepsilon}_{min}$ [5]

$$\dot{\varepsilon}_{min} = A_c \sigma^{n_c} \exp\left(-\frac{Q_c}{kT}\right) \quad (6)$$

The apparent activation energy, Q_f, exceeds the value of the activation enthalpy of lattice diffusion $\Delta H_D = 142$ kJ mol^{-1}, namely $Q_f \in (1.8–2.2)\Delta H_D$. The values of n_f and Q_f can be compared with those obtained for similar dispersion-strengthened alloys produced in the laboratory of Professor Jangg at the Technical University of Vienna (Al–2.5% Al_4C_3–2.1% Al_2O_3(vol %), $n_f = 18.4 \pm 1.0$, $Q_f = 247 \pm 19$ kJ mol^{-1}; Al–10% Al_4C_3–3.8% Al_2O_3(vol %), $n_f = 18.1 \pm 0.8$, $Q_f = 264 \pm 18$ kJ mol^{-1} (derived from data in [13]). The activation energy, Q_f, is higher

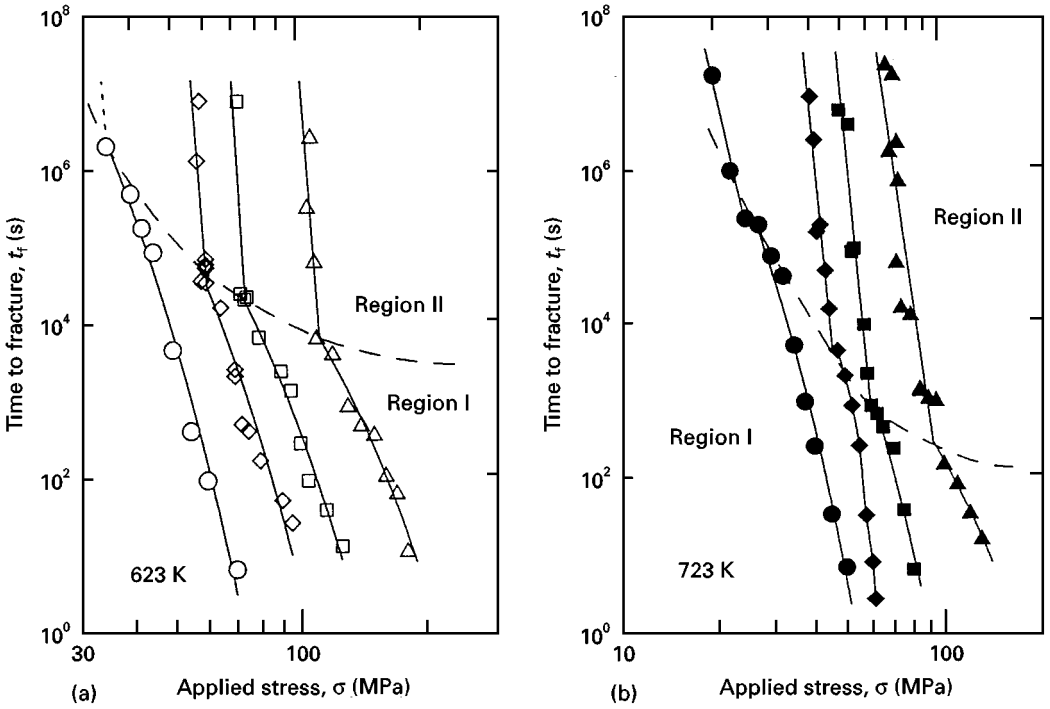

Figure 4 Stress dependence of time to fracture. (a) 623 K, (b) 723 K. (○, ●) AlC0, (◇, ◆) AlC1, (□, ■) AlC2, (△, ▲) AlC2O2.

TABLE I Calculated values of stress sensitivity and activation energy of time to fracture

Alloy	n_f	Q_f (kJ mol^{-1})
AlC0	16.83 ± 0.82	249.8 ± 20.2
AlC1	24.06 ± 1.86	314.1 ± 32.3
AlC2	21.26 ± 2.17	287.8 ± 41.5
AlC2O2	19.85 ± 1.90	260.3 ± 41.2

for AlC2 than for the alloy studied by Matsuda and Matsuura [11]. Owing to the scarcity of temperature values in the present paper, the importance of this result need not be overestimated.

A detailed inspection of the time-to-fracture data suggests the existence of two regions (see Fig. 4). At higher stress levels (Region I) the data are better described by the exponential function, whereas at lower stress (Region II) the data can be fitted by the power function. The values of the power in the low stress region are extremely high ($n_f > 80$ at 623 K and $n_f > 50$ at 723 K). The stress at which a transition is observed decreases with increasing temperature and volume fraction of the secondary phase. The proposed division corresponds closely to that reported for the Inconel alloy MA6000 by Benn and Kang [14].

Fig. 5 shows the stress dependence of the strain at fracture. Formally, the dependence can be described by an equation analogous to Equation 5. The strain to cause fracture can be better correlated with the minimum creep rate. Fig. 6 shows an example. At low creep rates, the fracture strain is low, and it is independent of the creep rate. (Perhaps it is slowly decreasing with increasing creep rate.) At high creep rates, the fracture strain grows with the creep rate. The critical creep rate at which a transition between the two regimes occurs is higher, the higher are the temperature and the volume fraction of the secondary phase. The boundary between the two regions is approximately the same for the strain-to-fracture behaviour as for the time to the occurrence of fracture.

4. Discussion

4.1. Description of the tertiary stage of creep curves

The parameter C in Equation 3 correlates reasonably well with the reciprocal value of the strain to fracture as shown in Fig. 7. The dependence can be described simply by

$$C\varepsilon_f = 3.92 \pm 1.83 \quad (7)$$

The same relation has also been reported for the tertiary stage of creep curves in three molybdenum and CrMo-steels [10]. The parameter C is, in fact, the slope of the creep curve in coordinates $\ln \dot{\varepsilon}$ versus ε. This means that the logarithmic increment of the creep rate during the tertiary creep is a constant, independent of the external conditions and the composition of the alloy

$$\ln \dot{\varepsilon}_f - \ln \dot{\varepsilon}_{min} = C\varepsilon_f \quad (8)$$

wherein $\dot{\varepsilon}_f$ is the creep rate at fracture. Because the secondary phases in the alloys are very stable, the increased creep rate in the tertiary stage has to be attributed to the reduction of the effective cross-section of the test specimens caused by the formation of internal defects such as cavities or cracks. (The reduction of the cross-section due to the plastic deformation is compensated by the loading system.) The applied stress dependence of the creep rate is governed by a power law (*cf.* Equation 6) and therefore the logarithmic increment of the applied stress is

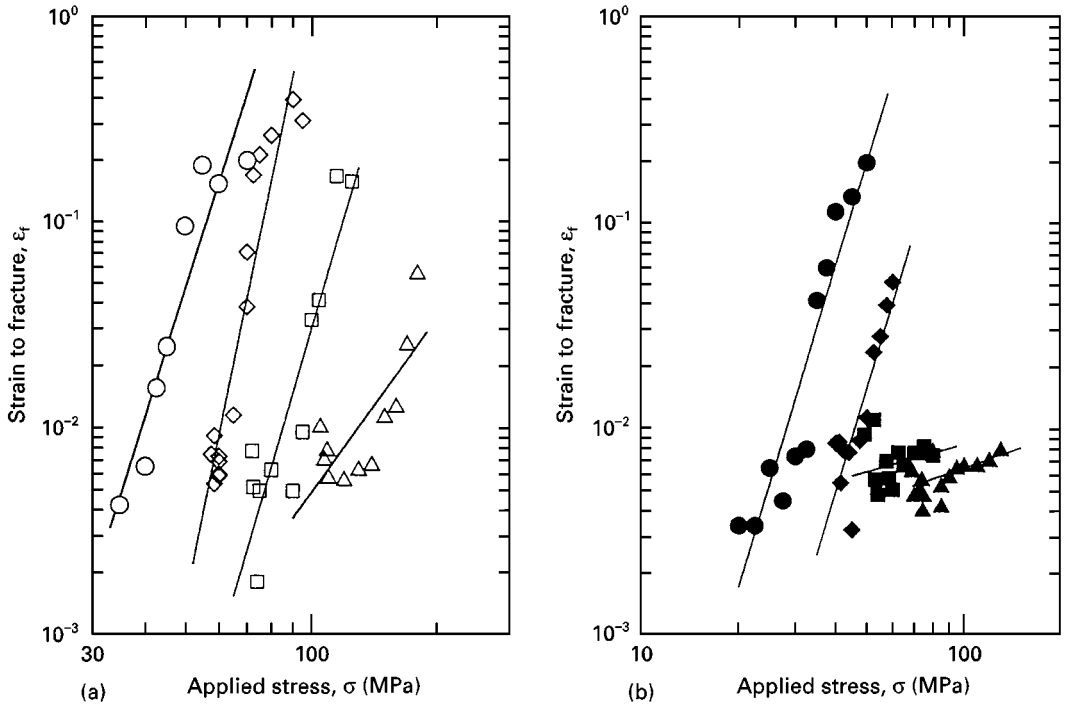

Figure 5 Stress dependence of strain to fracture. (a) 623 K, (b) 723 K. (○, ●) AlC0, (◇, ◆) AlC1, (□, ■) AlC2, (△, ▲) AlC2O2.

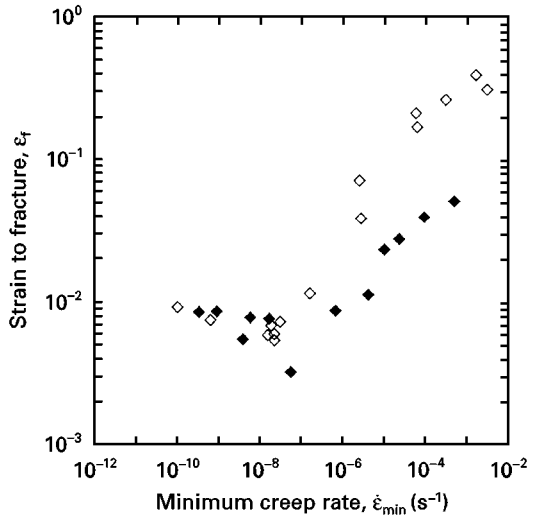

Figure 6 Dependence of strain to fracture on minimum creep rate, for AlC1 at (◇) 623 K and (◆) 723 K.

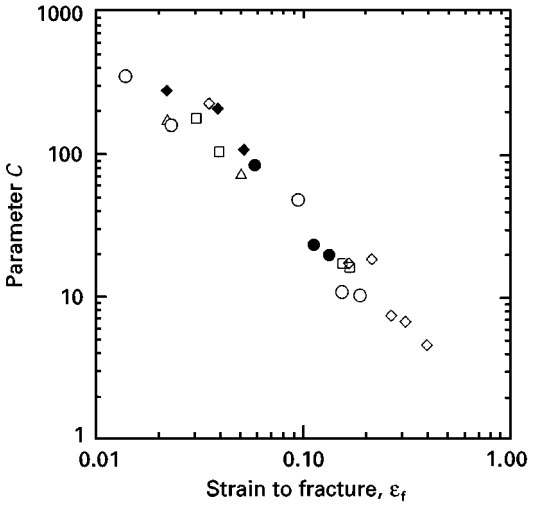

Figure 7 Dependence of parameter C on strain to fracture, at (○, ◇, □, △) 623 K, and (●, ◆) 723 K, for (○, ●) AlC0, (◇, ◆) AlC1, (□) AlC2, (△) AlC2O2.

also a constant

$$\ln \sigma_f - \ln \sigma = \frac{C\varepsilon_f}{n_c} \quad (9)$$

where σ_f is the effective stress acting at fracture. This suggests that the critical condition for fracture is given by the achievement of a critical fraction of damaged area in a cross-section

$$f_c = 1 - \exp\left(-\frac{C\varepsilon_f}{n_c}\right) \quad (10)$$

rather than by, for example, critical stress. The critical fraction, f_c, calculated by means of the data presented in Fig. 7 and n_c from a previous paper [5] equals 0.139 ± 0.056.

In Equation 2, the reciprocal value of parameter θ_4 can be interpreted as the characteristic relaxation time of the tertiary creep, τ_3. It may be interesting to compare this with the analogical quantity for the primary creep, i.e. τ_1 in the term [5] $\varepsilon_1(1 - \exp[-t/\tau_1])$, wherein ε_1 is the limiting primary strain. This is illustrated for the alloy AlC0 in Fig. 8. The values of τ_1 and τ_3 can be extrapolated one to another. This agreement justifies a modification of the theta projection concept (with $\theta_2 = 1/\tau_1 = \theta_4$) proposed by Maruyama *et al.* [15].

4.2. Relationship between the creep rate and the time to fracture

The close resemblance of the characteristic features of the primary and tertiary stages of creep implies

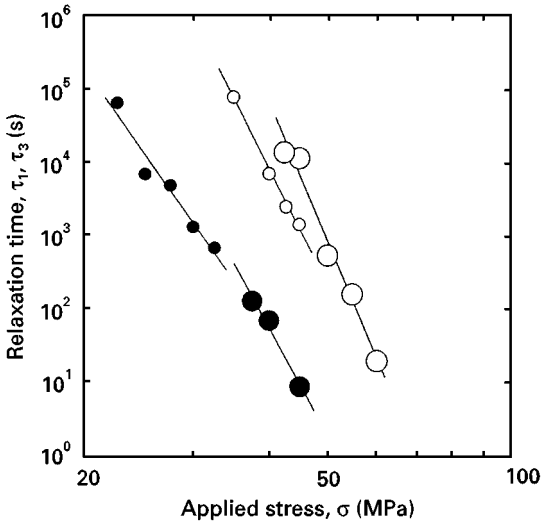

Figure 8 Stress dependence of relaxation times of primary and tertiary creep in the alloy AlC0, at (○, ○) 623 K and (●, ●) 723 K, for (○, ●) τ_1, (○, ●) τ_3.

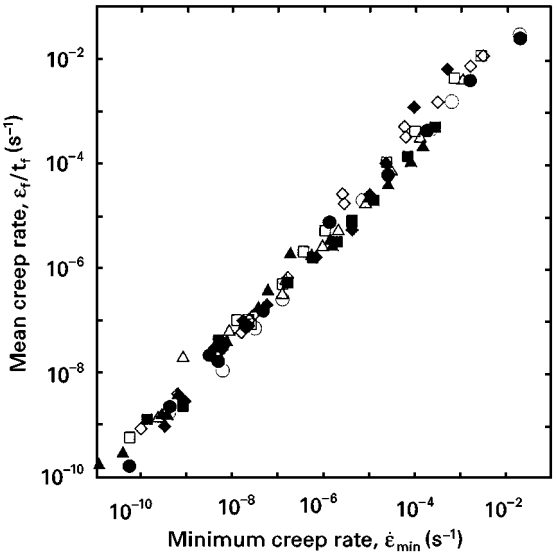

Figure 9 A modified Monkman–Grant plot showing the dependence of mean creep rate on minimum creep rate, at (○, ◇, □, △) 623 K, and (●, ◆, ■, ▲) 723 K, for (○, ●) AlC0, (◇, ◆) AlC1, (□, ■) AlC2, (△, ▲) AlC2O2.

correspondence of the deformation and fracture processes in the creep of the alloys studied. As was shown in the preceding section, the dominant role of void formation in the tertiary creep must not be neglected. The observed correspondence thus indicates that the void formation is controlled by deformation processes rather than by diffusional growth. This can be further supported by the relationship between the minimum creep rate and the time to the occurrence of fracture [16]. The modified Monkman–Grant equation yields a better correlation of these quantities [17]

$$\dot{\varepsilon}_{min} t_f/\varepsilon_f = \text{const.} \quad (11)$$

The data for the alloys are summarized in Fig. 9. The proportionality constant is equal to 0.292 ± 0.160. Equation 11 is valid irrespective of different features of tertiary creep and fracture appearance at low and high stress. By inserting the fracture condition $\varepsilon = \varepsilon_f$ for $t = t_f$, Equation 3 can be rearranged as follows

$$\dot{\varepsilon}_{min} t_f/\varepsilon_f = [1 - \exp(-C\varepsilon_f)]/(C\varepsilon_f) \quad (12)$$

The reciprocal dependence of the parameter C and the strain to fracture can thus substantiate the modified Monkman–Grant equation. Using Equation 7, the right-hand side of Equation 12 equals 0.250. This agrees with the constant determined for the modified Monkman–Grant equation (0.274 ± 0.127 if the identical data are considered).

The correspondence of deformation and fracture processes may offer a possible explanation of the observed regions in the time-to-fracture behaviour. This follows the ideas of Raj [18]. At low stresses, the deformation of the alloys is determined by the creep of the dispersoid, and the stress sensitivity is high, owing to the proximity of the threshold stress. At stresses greater than the Orowan stress, the dominant role in deformation is ascribed to the matrix. Because the Orowan stress is greater than the power-law breakdown ($\sim 5 \times 10^{-4} G$, G being the Young's modulus), exponential behaviour is to be expected.

4.3. Transition between low and high creep ductilities

Similar characteristics of the transition between the low and the high ductility areas illustrated in Fig. 6 were reported by Pandey *et al.* [12] for the creep fracture behaviour of Al–SiC composites. Pandey *et al.* suggested that the fracture in the high-ductility region occurred by nucleation of cavities at intragranular particles. Consequently, they tried to identify the transition with the criteria of cavity nucleation given by Koeller and Raj [19] and by Brown and Stobbs [20].

According to Koeller and Raj [19], the critical strain rate is given by

$$\dot{\varepsilon}^{crit} = 118 \frac{(1-\nu)(1-2\nu+2/\pi)}{(5/6-\nu)^2} \frac{G\Omega}{kT} \frac{f_v \delta D_B}{p^3} \quad (13)$$

wherein ν is the Poisson's ratio, δ the grain-boundary width, D_B the grain-boundary diffusion coefficient, Ω the atomic volume, f_v the volume fraction of dispersed particles, and p the particle diameter. Using the grain-boundary diffusivity estimated by Koeller and Raj ($\delta D_B = 5 \times 10^{-14} \exp[-84\,000/(8.31\,T)]$) the calculation reveals a critical strain rate many orders of magnitude greater than that observed experimentally. Moreover, according to this theory, the ductility should be enhanced at subcritical strain rates where the rate of straining is slower than the rate of stress relaxation. The same objection is also valid for the experimental observations of Pandey *et al.* [12] on Al–SiC metal-matrix composites. It seems likely that the critical strain rate given by Equation 13 corresponds to another boundary, e.g. a middle regime of superplastic behaviour [21].

Another criterion for cavity nucleation in aluminium composites was published by Brown and Stobbs [20]. They gave the minimum critical strain necessary

for the onset of plastic cavitation as

$$\varepsilon_c \geqslant \frac{3\gamma}{G\boldsymbol{b}} \tag{14}$$

wherein γ is the surface energy and $\boldsymbol{b}$ is the Burgers vector length. Using $\gamma = 1\,\mathrm{N\,m^{-1}}$, $\boldsymbol{b} = 2.86 \times 10^{-10}\,\mathrm{m}$, this critical strain is of the order of 0.5 and thus substantially higher than the strain corresponding to the transition between low and high creep ductilities.

5. Conclusions

1. The increment of logarithm of the creep rate in the tertiary stage is a constant, independent of the external conditions. This indicates that the condition for fracture is given by the achievement of a critical fraction of the damaged area.

2. The description of the tertiary stage of creep by the logarithmic function validates the modified Monkman–Grant equation.

3. The relaxation time of the tertiary creep can be extrapolated to the same quantity for the primary creep. This suggests that the processes in the primary and the tertiary creep may be governed by the same mechanism. This fact is further supported by the modified Monkman–Grant equation.

4. Although the characteristic of the transition between the areas of low and high ductility are in qualitative agreement with the strain-rate criterion published by Koeller and Raj [19], the present experimental data cannot be explained by this theory.

Acknowledgements

The paper is based on work supported partly by the Grant Agency of the Academy of Sciences under grant no. A2041502 and by the Grant Agency of the Czech Republic under grant no. 106/95/1530. The author thanks his colleagues Dr K. Kuchařová and Dr K. Milička for providing some experimental results.

References

1. J. S. BENJAMIN, *Metall. Trans.* **1** (1970) 2943.
2. G. JANGG, F. KUTNER and G. KORB, *Aluminium* **51** (1975) 641.
3. E. ARZT, *Res. Mechanica* **31** (1991) 399.
4. A. H. COTTRELL, "Structural Processes in Creep", Iron and Steel Institute Special Report 70 (Iron and Steel Institute, London, 1961) p. 1.
5. F. DOBEŠ, K. KUCHAŘOVÁ, A. ORLOVÁ, K. MILIČKA and J. ČADEK, *Mater. Sci. Engng* **A174** (1994) 37.
6. *Idem., Acta Metall. Mater.* **42** (1994) 1447.
7. T. HOSTINSKÝ and J. ČADEK, *J. Test. Eval.* **4** (1976) 26.
8. A. GRAHAM and K. F. A. WALLES, *J. Iron Steel Inst.* **179** (1955) 105.
9. R. W. EVANS and B. WILSHIRE, "Creep of Metals and Alloys" (The Institute of Metals, London, 1985).
10. R. SANDSTRÖM and A. KONDYR, in "Proceedings of the 3rd International Conference on Mechanical Behaviour of Materials", Vol. 2, edited by K. J. Miller and R. F. Smith (Pergamon Press, Oxford, New York, 1980) p. 275.
11. M. MATSUDA and K. MATSUURA, in "Proceedings of MRS International Meeting Advanced Materials", edited by M. Doyama (Materials Research Society, Pittsburgh, PA, 1989) p. 73.
12. A. B. PANDEY, R. S. MISHRA and Y. R. MAHAJAN, *J. Mater. Sci.* **28** (1993) 2943.
13. A. ORLOVÁ, K. KUCHAŘOVÁ, J. ČADEK, M. BESTERCI and M. ŠLESÁR, *Kovové Materiály* **24** (1986) 505.
14. R. C. BENN and S. K. KANG, in "Superalloys 1984", edited by M. Gell, C. S. Kortovich, R. H. Bricknell, W. B. Kent and J. F. Radavich (TMS-AIME, Warrendale, PA, 1984) p. 319.
15. K. MARUYAMA, CH. HARADA and H. OIKAWA, *Trans. Iron Steel Inst. Jpn* **26** (1986) 212.
16. F. C. MONKMAN and N. J. GRANT, *Proc. ASTM* **56** (1956) 593.
17. F. DOBEŠ and K. MILIČKA, *Metal. Sci.* **10** (1976) 382.
18. S. V. RAJ, in "Mechanical Properties of Metallic Composites", edited by S. Ochiai (Marcel Dekker, New York, 1994) p. 97.
19. R. C. KOELLER and R. RAJ, *Acta Metall.* **26** (1978) 1551.
20. L. M. BROWN and W. M. STOBBS, *Philos. Mag.* **34** (1976) 351.
21. T. R. BIELER, G. R. GOTO and A. K. MUKHERJEE, *J. Mater. Sci.* **25** (1990) 4125.

Received 5 July 1996
and accepted 27 January 1998